

1 **District-level healthcare accessibility under flood-conditioned road network disruption in**
2 **Pakistan**

3 Ramla Khan^{*1}, Martin Lauer², Muhammad Marwan³

4 1 Health Data Sciences, The University of Oxford, United Kingdom

5 ²NDORMS (Nuffield Department of Orthopaedics, Rheumatology and Musculoskeletal Sciences), IT Services, The University of Oxford,
6 United Kingdom

7 ³School of Mathematics and Statistics, Linyi University, China

8 *email: ramla.khan@ndorms.ox.ac.uk; ramla3903@gmail.com

9
10
11 **Abstract**

12 Floods disrupt healthcare access not only through facility damage but through road network fragmentation. This
13 study quantifies district-level healthcare accessibility loss during the 2025 monsoon floods in Sindh and Punjab,
14 Pakistan, using a flood-conditioned weighted road network model that reveals how network topology, rather
15 than facility availability, governs access collapse. Satellite-derived flood extents were integrated with road
16 network, healthcare facility, and demographic data; segments with $\geq 60\%$ inundation was classified as unusable.
17 Shortest-path distances from facilities to district headquarters were computed at 5, 10, and 15 km thresholds.
18 Although only 0.6% of major road segments became unusable, their disruption at structurally critical locations
19 fragmented connectivity across entire districts, producing accessibility losses disproportionate to the physical
20 damage sustained. At the 5 km threshold, 84.8% of facilities in Sindh and 75.9% in Punjab were inaccessible,
21 with primary care facilities most severely affected. These findings demonstrate that protecting a small number of
22 critical road corridors could substantially preserve healthcare access during flood events.

23 **Keywords:** Flood impacts; Healthcare accessibility; Spatial network analysis; Road network disruption; Health
24 system resilience; Pakistan

25

26 **1 Introduction**

27 Floods rank among the most frequent and destructive natural hazards globally, disproportionately affecting
28 vulnerable communities and critical infrastructure [1]. Pakistan experiences recurring catastrophic floods,
29 including the 2010 event that claimed 1,985 lives and affected 20 million people [2] and the 2022 monsoon
30 floods, which impacted 33 million people and resulted in combined damages exceeding \$30 billion [3]. The
31 2025 monsoon floods, beginning in late June, claimed nearly 1,000 lives, displaced over one million people, and
32 destroyed thousands of homes, demonstrating persistent flood vulnerability despite ongoing adaptation efforts
33 [4].

34 Climate change has intensified flood risk across the Indus Basin through altered precipitation patterns,
35 accelerated glacial melt, and modified hydrological regimes [5,6]. Concurrent rapid urbanisation has
36 compounded this vulnerability, with impervious surface expansion significantly increasing pluvial flood severity
37 during high-intensity rainfall events [7]. These compound pressures create conditions in which concentrated
38 monsoon rainfall overwhelms existing drainage infrastructure and water management systems.

39 Floods generate cascading impacts beyond immediate physical destruction. Hydrological disturbances combined
40 with land-use change degrade groundwater quality, soil vitality, and ecosystem health [8,9]. Machine learning-
41 based mapping of the 2022 floods estimated that approximately ten million people and hundreds of thousands of
42 buildings were directly affected, with widespread cropland inundation disrupting rural livelihoods [10,11]. Such
43 disruptions weaken community resilience while straining fragile health systems.

44 Despite advances in hydrological modelling and environmental impact assessment, critical knowledge gaps
45 remain regarding flood impacts on healthcare infrastructure accessibility. High-resolution demographic datasets
46 and healthcare facility geolocation data enable unprecedented spatial precision in population exposure
47 assessment [12], yet these resources remain underutilised for evaluating health system disruption during flood
48 events. Similarly, remote-sensing-based flood products allow precise spatiotemporal inundation mapping [13],
49 but their application to healthcare accessibility analysis is limited.

50 This study addresses these gaps by integrating demographic, healthcare, and remote-sensing data to quantify
51 healthcare facility accessibility during the 2025 Pakistan floods. Specifically, we assess flood impacts on road
52 network connectivity using high-resolution inundation data, calculate network-based distances from district
53 headquarters (DHQ) to healthcare facilities under flood conditions, and classify facility accessibility at multiple
54 distance thresholds. This approach provides spatially explicit evidence of health system vulnerability to inform
55 disaster preparedness and response planning.

56 This study advances existing research by providing a district-level assessment of healthcare accessibility under
57 flood conditions, integrating high-resolution flood extent data with network-based accessibility modelling.
58 Unlike previous studies that focus on direct flood exposure or general accessibility measures, this approach
59 demonstrates how limited disruption to strategically important road segments can result in disproportionate
60 losses in healthcare access due to underlying network structure.

61 2 Methods

62 The analytical workflow followed a structured sequence of four stages: (1) flood extent integration and road
63 exposure assessment, (2) road network pre-processing and construction of a flood-conditioned network, (3)
64 network-based distance calculation between healthcare facilities and DHQ, and (4) accessibility classification
65 and district-level aggregation. This framework enables the systematic evaluation of how flood-induced road
66 disruption affects healthcare accessibility.

67 All spatial analyses were conducted in R version 4.3.0 (R Core Team, 2023) using sf [14,15] for spatial vector
68 operations, terra [16] for raster processing, sfnetworks [17] for network graph construction and analysis, and
69 dplyr [18] and tidyr [19] for data manipulation. Statistical tests employed the base R stats package [20]. Map
70 production and cartographic visualisation were performed in QGIS version 3.40.9 [21]

71 2.1 Study Area

72 Punjab Province and a broader region covering Sindh Province were analysed in this study. They represent
73 Pakistan's flood-vulnerable districts within the Indus Basin system. A 50 km buffer was applied around the
74 union of both flood extents to capture road network connectivity beyond the immediate inundation zone,
75 allowing analysis of alternative routes and network effects outside directly flooded areas.

76 2.2 Data Sources

77 Flood extent data were obtained from the United Nations Satellite Centre (UNOSAT) as binary raster layers at
78 20 m spatial resolution, indicating inundated areas. The Punjab scenario [22] and the Sindh scenario [23]
79 represent peak flood conditions during the 2025 monsoon season during the first half of July, derived from
80 Sentinel-1 Synthetic Aperture Radar (SAR) and Multispectral Sentinel-2 imagery.

81 Road network data were extracted from OpenStreetMap (OSM) [24]. The dataset includes spatial geometries,
82 highway classifications, and attributes such as road names and lane count where available.

83 Healthcare facility locations (point features) were obtained from OSM [25]. Facilities include diverse categories
84 ranging from Basic Health Units (BHU) and Rural Health Centres (RHC) to DHQ Hospitals and specialised
85 facilities.

86 Administrative boundaries at the district level (Level 2) were obtained from the World Food Programme Spatial
87 Data Infrastructure [26], quality-assured by OCHA Field Information Services.

88 Demographic data was acquired from WorldPop [12], as multiple raster images, each representing age groups of
89 male or female gender.

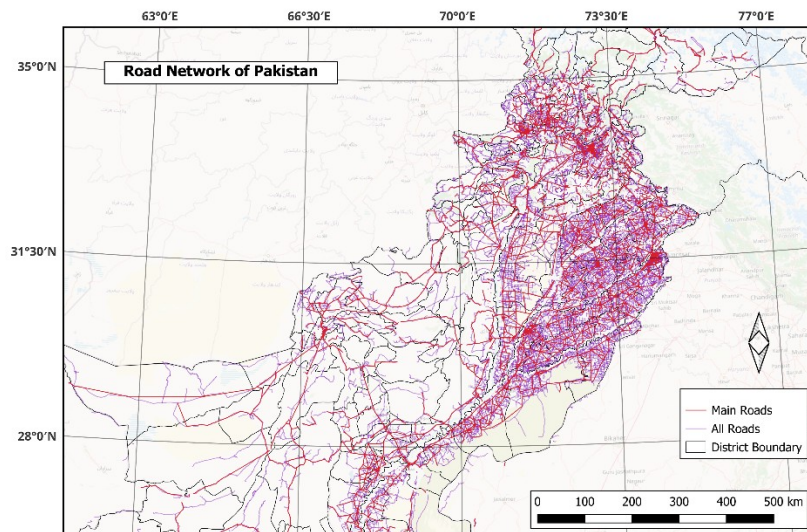
90 This study relies on secondary spatial datasets, including satellite-derived flood extents (UNOSAT), OSM
91 infrastructure data, and WorldPop demographic grids, which are widely used in large-scale disaster and
92 accessibility analyses. Similar approaches have been applied in recent studies assessing flood-induced disruption
93 to healthcare access and critical infrastructure [27,28]. While field validation was not feasible given the spatial
94 extent of the study, the integration of multiple independent datasets enhances the robustness and consistency of
95 the analysis.

96 **2.3 Spatial Data Processing**

97 All spatial datasets were verified for coordinate reference system (CRS) consistency and projected to UTM
98 Zone 42N (EPSG:32642) for accurate distance calculations. Spatial extents of roads, healthcare facilities, and
99 districts were cropped to a 50 km buffer around the union of both flood scenario extents. This buffer ensures the
100 analysis captures potential route diversions around flooded areas while excluding distant infrastructure unlikely
101 to influence district-level accessibility during the flood event.

102 **2.4 Road Network Preparation**

103 Road network pre-processing was performed to ensure topological validity and computational efficiency. Only
104 major road classifications supporting inter-district connectivity and emergency response were retained,
105 including primary, secondary, trunk, motorway, and highway classes, along with their associated link roads (Fig.
106 1). Minor road types such as residential streets, service roads, and tracks were excluded.



107

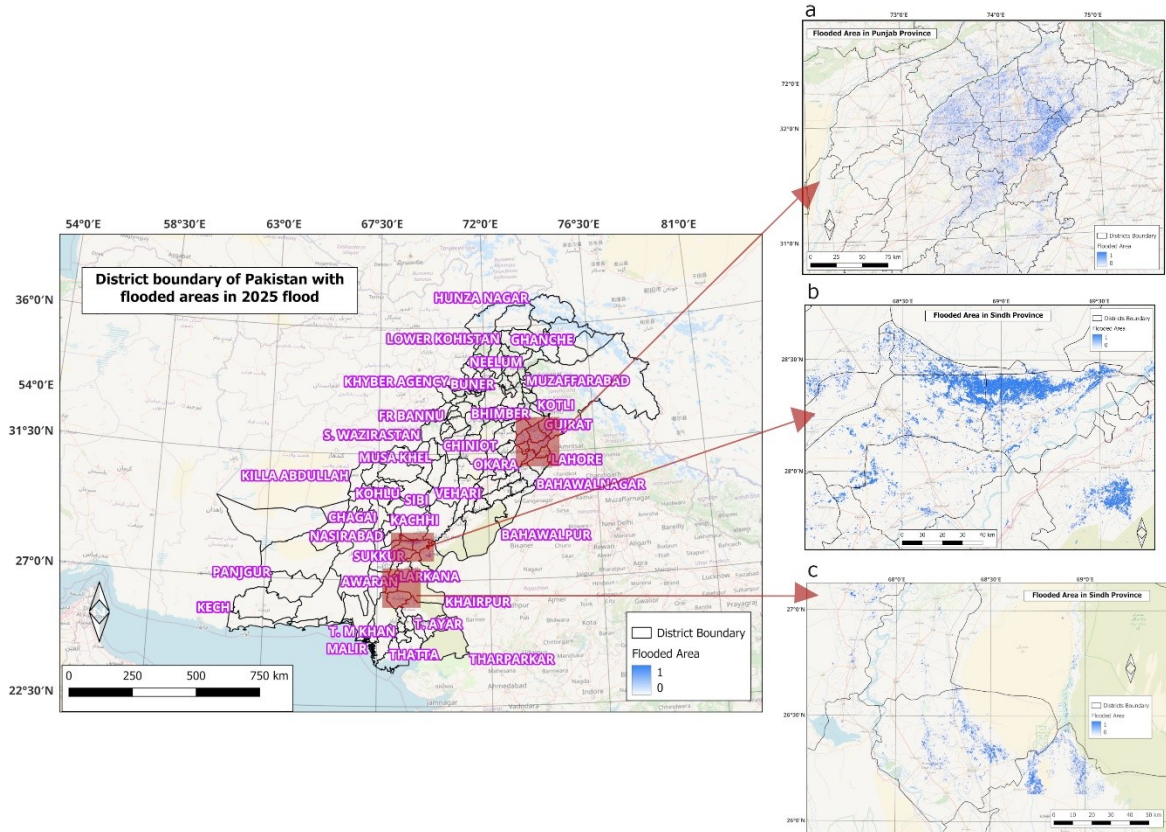
108 *Fig. 1. Road network of Pakistan with main roads represented with magenta colour, while the thinner purple*
109 *lines represent all roads, inclusive of residential streets, service roads, and tracks.*

110 Duplicate road segments with identical geometries were removed to prevent redundancy in network analysis.
111 Invalid geometries were corrected using standard validation procedures. Road features stored as Multiline-String
112 geometries were converted to individual Line-String segments to ensure each segment functions as a single
113 network edge. Segments shorter than 5 m were removed as digitisation artefacts that could introduce spurious
114 network nodes. Following these pre-processing steps, unique identifiers were assigned to all retained segments,
115 and segment lengths were calculated in meters for use as edge weights in network analysis.

116 The pre-processing reduced the road network from its original size to a cleaned dataset suitable for graph-based
117 analysis. Road type distribution was verified to ensure adequate representation of major road classes. Total road
118 length in the study area was calculated as the sum of all segment lengths.

119 2.5 Flood Impact Assessment

120 The combined flood raster was created by loading both the Punjab and Sindh flood raster, stacking them, and
121 applying a pixel-wise maximum function to produce a unified binary inundation surface. This combined raster
122 was used for all subsequent flood impact assessments (Fig. 2).



123

124 *Fig. 2. Flooded areas of Pakistan in the summer of 2025 a) Punjab province, b) Northmost Sindh, c) the middle*
125 *of Sindh*

126 Road flood exposure was assessed using a point-based sampling approach rather than computationally
127 expensive raster-to-polygon conversion. Sample points were generated along each road segment at 20 m
128 intervals, matching the spatial resolution of the flood raster. This sampling density ensures adequate
129 representation of flood conditions along each segment while maintaining computational feasibility.

130 Flood values were extracted from the combined flood raster at each sample point location. Points intersecting
131 flooded raster cells (value = 1) were classified as flooded, while those intersecting non-flooded or no-data cells
132 (value = 0 or NA) were classified as non-flooded. For each road segment, the percentage of sample points
133 classified as flooded was calculated, providing a continuous measure of inundation severity.

134 Road segments were classified as unusable if 60% or more of their sampled length was flooded. This threshold
135 provides a segment-level approximation of loss of operability under flood conditions and reflects functional
136 disruption for emergency and service vehicles. Previous studies have demonstrated that even partial inundation
137 can significantly impair road usability depending on flood depth and vehicle type [29,30]. Sensitivity testing
138 using alternative thresholds (50% and 70%) produced qualitatively similar spatial patterns, supporting the
139 robustness of the selected threshold.

140 **2.6 Network Construction and Accessibility Analysis**

141 Usable road segments were assembled into a weighted, undirected network graph. Nodes represent road
142 intersections and segment endpoints, while edges represent road segments weighted by their length in meters.
143 Road segments classified as unusable due to flooding were excluded, producing a flood-conditioned network
144 representing viable travel paths during the event.

145 DHQ served as origin points for accessibility analysis, reflecting their role as administrative hubs and focal
146 points for healthcare coordination and emergency response during flood events. This approach is consistent with
147 prior accessibility studies in low- and middle-income settings that model access relative to key service or
148 administrative centres [31]. District polygon centroids were used to represent headquarters locations, reflecting
149 their typical role as administrative hubs and centres for healthcare coordination and emergency response. All
150 district centroids were snapped to their nearest node in the flood-conditioned road network to enable accurate
151 distance calculations.

152 Healthcare facilities were similarly snapped to their nearest network node. Network distances were calculated
153 using Dijkstra's shortest path algorithm [32–34], computing the minimum cumulative edge weight (in meters)
154 along the flood-conditioned network from each facility to all DHQ. For each facility, the nearest accessible
155 DHQ and corresponding network distance were recorded. Facilities with no valid path to any DHQ were
156 assigned an infinite distance, indicating complete network disconnection.

157 **2.7 Accessibility Classification**

158 Healthcare facilities were classified using three distance thresholds representing different accessibility contexts:
159 5 km (short-range, typical of urban and peri-urban settings), 10 km (medium-range, representing suburban and
160 accessible rural areas), and 15 km (extended-range, capturing more remote rural contexts). The 5 km threshold
161 is widely recognised in healthcare accessibility studies in low- and middle-income countries (LMICs) as a
162 benchmark for reasonable access to care [35,36], while larger thresholds capture reduced service availability in
163 peri-urban and rural areas. Healthcare utilisation declines with increasing distance, reflecting a well-established
164 distance-decay effect in access to services [31]. The use of multiple thresholds allows accessibility to be
165 evaluated across varying spatial contexts and levels of service availability, consistent with previous flood-related
166 accessibility analyses [27].

167 For each threshold, facilities were classified into three mutually exclusive categories. Facilities were classified
168 as accessible if a valid network path existed and the distance to the nearest DHQ was less than or equal to the
169 threshold. Facilities were classified as inaccessible if a valid network path existed, but the distance exceeded the
170 threshold. Facilities were classified as disconnected if no valid network path existed due to complete network
171 severance, representing the most critical condition from an emergency response perspective.

172 Binary accessibility indicators were created for each threshold (5 km, 10 km, 15 km), and categorical status
173 variables were assigned based on the distance and connectivity criteria. Summary statistics were generated by
174 facility category, distance threshold, and accessibility status to quantify the number and percentage of facilities
175 in each classification.

176 2.8 Statistical Analysis

177 Descriptive statistics were used to summarise healthcare facility accessibility outcomes across distance
178 thresholds (5 km, 10 km, and 15 km) by facility category, district, and province. Facility accessibility status was
179 classified as accessible, inaccessible, or disconnected based on flood-conditioned network distances to the
180 nearest DHQ.

181 To assess whether observed differences in accessibility patterns departed from random variation, chi-square tests
182 of independence with Monte Carlo simulation (10,000 replicates) were conducted [37]. Tests were applied in
183 two contexts. First, associations between healthcare facility category and accessibility status were evaluated to
184 examine whether accessibility loss differed systematically by level of care. Second, accessibility status
185 distributions were compared across provinces at each distance threshold to assess whether province-level
186 differences were statistically distinguishable.

187 Monte Carlo simulation was employed to avoid reliance on asymptotic assumptions given small and uneven cell
188 counts in certain facility categories and districts. Effect sizes were assessed using Cramér's V to support the
189 interpretation of statistically significant results. Statistical analyses were performed in R, with results interpreted
190 as confirmatory evidence supporting descriptive and spatial patterns rather than as primary inferential outcomes.

191 3 Results

192 3.1 Flood-Exposed Population by Age and Sex

193 Flood exposure analysis indicates substantial demographic impacts across Sindh and Punjab provinces (Table 1;
194 Fig. 3). An estimated 1.22 million people resided within the mapped flood extents, with Punjab accounting for
195 approximately 67% of the exposed population (820,950 individuals) and Sindh contributing the remaining 33%
196 (398,084 individuals).

197 Across both provinces, flood exposure was concentrated among children and working-age adults. Individuals
198 aged 0–14 years constituted 25.1% of the exposed population in Sindh and 27.4% in Punjab. The largest
199 absolute exposure occurred in the 15–34 age range in both provinces, reflecting underlying population structure
200 and the spatial coincidence of densely inhabited districts with flood-prone areas.

201 Sex-disaggregated estimates showed broadly balanced exposure patterns. Males represented 51.1% of the
202 exposed population in Sindh and 50.1% in Punjab, with minimal differences between sexes across most age
203 groups (Table 1). Minor deviations were observed in older age cohorts, where female exposure slightly
204 exceeded male exposure.

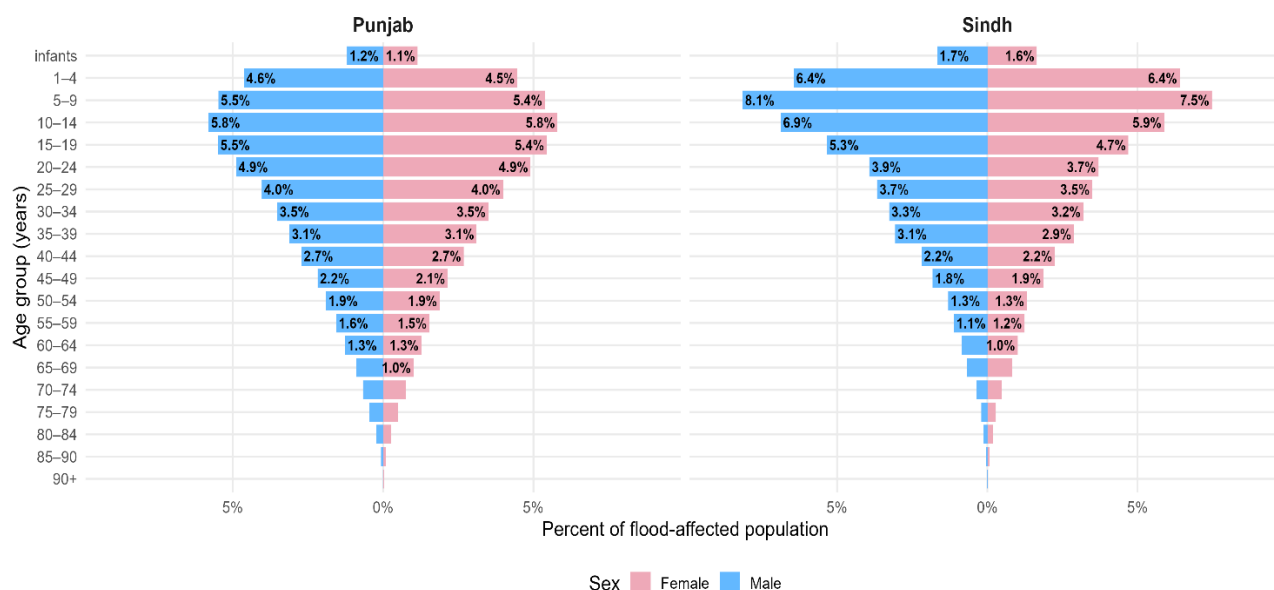
205 Population pyramids illustrate similar age–sex structures of flood-exposed populations in both provinces,
206 characterised by wide bases and progressively narrowing upper age bands (Fig. 3). Individuals aged 60 years
207 and older accounted for a smaller proportion of total exposure relative to younger age groups in both Sindh and
208 Punjab.

209 *Table 1. Estimated population counts derived from a gridded population raster (100 m resolution) intersected*
210 *with the flood extent in the Punjab and Sindh provinces of Pakistan in 2025.*

Age group (years)	Sindh Female	Sindh Male	Sindh Total	Punjab Female	Punjab Male	Punjab Total
infants	6,584	6,630	13,214	9,451	9,834	19,285
1–4	25,501	25,640	51,142	36,608	38,032	74,640

5–9	29,740	32,384	62,124	44,106	44,920	89,026
10–14	23,406	27,375	50,781	47,640	47,656	95,296
15–19	18,676	21,256	39,932	44,652	45,047	89,699
20–24	14,739	15,646	30,385	40,290	40,146	80,435
25–29	13,900	14,604	28,504	32,722	33,132	65,854
30–34	12,682	13,028	25,709	28,737	28,899	57,636
35–39	11,465	12,218	23,683	25,501	25,647	51,148
40–44	8,918	8,730	17,648	22,035	22,339	44,374
45–49	7,442	7,243	14,685	17,663	17,876	35,539
50–54	5,216	5,174	10,391	15,418	15,625	31,043
55–59	4,933	4,403	9,337	12,616	12,765	25,381
60–64	4,033	3,366	7,399	10,389	10,392	20,780
65–69	3,290	2,703	5,993	8,251	7,410	15,661
70–74	1,927	1,432	3,360	6,160	5,459	11,618
75–79	1,149	781	1,930	4,144	3,731	7,875
80–84	710	467	1,176	2,157	1,910	4,067
85–90	325	204	529	730	597	1,326
90+	104	58	162	159	104	264
All ages	194,741	203,343	398,084	409,430	411,520	820,950

211



212

213

214

Fig. 3. Population pyramids showing age-sex distribution of flood-exposed populations in Sindh and Punjab provinces of Pakistan in 2025.

215 3.2 Road Network Disruption Under Flood Conditions

216 Flood impact assessment revealed limited but spatially concentrated disruption to the major road network across
 217 the study area (Table 2). Of the retained road segments, approximately 0.6% were classified as unusable under
 218 flood conditions, corresponding to 40 individual segments and a total unusable length of 2.99 km.

219 All unusable segments were located within the primary set of major road corridors, while elevated structures
 220 such as viaducts were not affected. Low-water crossings were not identified as inundated in the dataset;
 221 however, this may reflect limitations in flood detection or spatial resolution rather than actual operability.

222 Although the total length of affected roads represented a small fraction of the overall network, unusable
223 segments were unevenly distributed and occurred at specific low-lying locations.

224 Lower-order connectors linking rural and peri-urban settlements to district centres were disproportionately
225 represented among unusable segments. Several districts experienced fragmentation of inter-district routes
226 despite limited overall road exposure, reflecting localised network disruption rather than widespread network
227 failure.

228 Full details of flood exposure and usability classification for all road segments are provided in Supplementary
229 Table S1.

230 *Table 2. Flood impact on different types of roads in the combined Sindh and Punjab*

Road classification	Total segments	Usable segments	Unusable segments	% unusable	Total length (km)	Unusable length (km)
Major road segments	6,948	6,908	40	0.6	679.36	2.99
Viaducts	85	85	0	0.0	37.18	0.00
Low-water crossings	2	2	0	0.0	0.06	0.00
Total	7,035	6,995	40	0.6	716.60	2.99

231

232 3.3 Spatial Distribution of Healthcare Facility accessibility

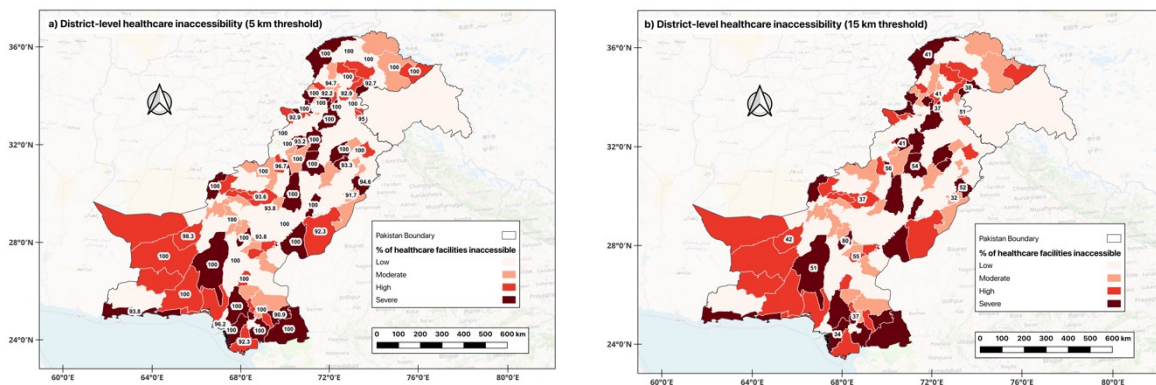
233 Spatial patterns of healthcare facility inaccessibility during the 2025 floods exhibited pronounced geographic
234 heterogeneity across both Sindh and Punjab provinces (Fig. 4; Supplementary Table S2, Supplementary Fig.
235 S1). Across all evaluated distance thresholds, accessibility loss was highly clustered at the district level rather
236 than uniformly distributed, reflecting differences in road network structure and redundancy. Districts with
237 limited alternative routes were more susceptible to disruption, where the loss of a small number of critical
238 segments resulted in disproportionate accessibility decline. The intermediate 10 km threshold exhibits similar
239 spatial patterns and is therefore presented in Supplementary Fig. S1.

240 At the 15 km threshold, inaccessibility was concentrated in a limited number of predominantly rural districts. In
241 Punjab, several districts recorded very high proportions of inaccessible facilities, while others experienced a
242 complete loss of accessibility within the threshold. In contrast, major urban and peri-urban districts retained full
243 accessibility despite geographic proximity to flood-affected areas, reflecting higher network redundancy and the
244 availability of multiple alternative routes.

245 A similar pattern was observed in Sindh, where districts in southern and interior regions exhibited consistently
246 high levels of inaccessibility at the 15 km threshold, whereas several central districts showed little or no
247 accessibility loss. Districts with both high proportions and large absolute numbers of affected facilities
248 accounted for a substantial share of total inaccessibility (Supplementary Table S2).

249 As distance thresholds were reduced, the spatial extent and severity of inaccessibility increased markedly,
250 reflecting the limited local connectivity of healthcare facilities in many districts. Short-range access was
251 particularly sensitive to network disruption, as even minor increases in travel distance resulted in facilities

252 exceeding lower accessibility thresholds. Additional districts transitioned from partial to majority
253 inaccessibility, particularly in rural settings where healthcare facilities are more sparsely distributed. At the 5 km
254 threshold, widespread accessibility loss was observed across both provinces, indicating severe constraints on
255 short-range access to district-level healthcare services under flood conditions.
256 Accessibility loss was not consistently related to the total number of facilities within districts, indicating that
257 connectivity, rather than facility density, was the dominant factor shaping accessibility outcomes under flood
258 conditions. Districts with relatively small facility inventories often experienced near-total inaccessibility, while
259 others with larger numbers of facilities retained access due to differences in network connectivity.
260 This pattern is consistent with previous studies demonstrating that disruption of a small number of strategically
261 located road segments can significantly reduce accessibility due to network topology effects [38].

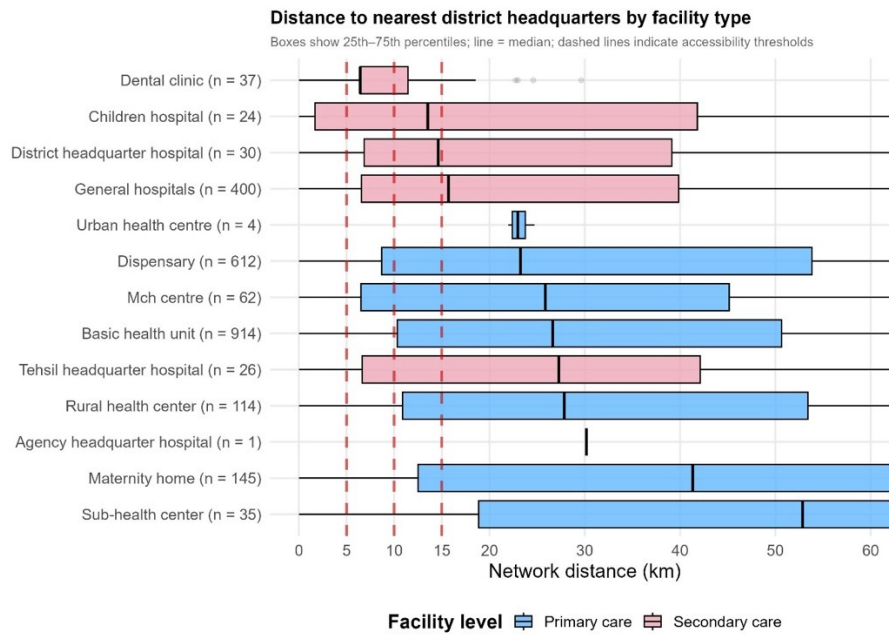


262 *Fig. 4. District-level healthcare inaccessibility under flood conditions in Sindh and Punjab: (a) 5 km threshold;*
263 *(b) 15 km threshold. Colours represent the percentage of healthcare facilities classified as inaccessible, with*
264 *darker shades indicating higher inaccessibility and clustering of severe impacts in districts with limited road*
265 *network connectivity.*

266 3.4 Network Distance to DHQ by Facility Type

267 Network distance distributions varied substantially by healthcare facility type under flood-conditioned road
268 connectivity (Fig. 5). Primary care facilities, including BHU, Dispensaries, RHC, and Sub-health Centres,
269 exhibited the largest median distances and widest interquartile ranges, with median distances frequently
270 exceeding 20–30 km and upper quartiles extending beyond 50 km.

271 In contrast, secondary and tertiary care facilities, such as District and Tehsil Headquarters Hospitals and
272 Children's Hospitals, were generally located closer to district centres, with median distances typically below 15
273 km. Dental clinics exhibited the shortest median distances, consistent with their predominantly urban
274 distribution.



275
276
277
278

Fig. 5. Network distances from healthcare facilities to the nearest DHQ under flood-conditioned road connectivity, stratified by facility type and level of care. Dashed vertical reference lines indicate accessibility thresholds at 5 km, 10 km, and 15 km.

279 3.5 Accessibility Loss Across Distance Thresholds

280 Aggregated province-level results indicated a consistent decline in the proportion of accessible facilities as
281 distance thresholds decreased (Fig. 5). At the 5 km threshold, 84.8% of facilities in Sindh and 75.9% in Punjab
282 were classified as affected. This proportion declined to 66.0% and 68.1% at the 10 km threshold, and to 62.5%
283 and 56.5% at the 15 km threshold, respectively.

284 Monte Carlo chi-square testing indicated that observed provincial differences were statistically distinguishable
285 at the 5 km threshold ($p = 0.002$), with a weak association strength (Cramér's $V = 0.11$). No statistically
286 significant differences were detected at the 10 km or 15 km thresholds ($p = 0.53$ and $p = 0.09$), indicating
287 convergence in accessibility outcomes as acceptable travel distances increased.

288 4 Discussion

289 A key contribution of this study is the demonstration that minimal physical disruption to road networks can
290 produce disproportionate losses in healthcare accessibility due to underlying network structure. While more
291 advanced network metrics such as centrality-based prioritisation frameworks have been applied in previous
292 studies, the present analysis focuses on distance-based accessibility to provide a scalable and interpretable
293 framework under data-constrained conditions.

294 This study provides a network-based assessment of healthcare accessibility during the 2025 monsoon floods in
295 Pakistan, revealing substantial and spatially uneven disruption across flood-affected districts. Although more
296 than one million people were exposed to flooding, the resulting loss of healthcare access was not uniformly
297 distributed across provinces or districts. Instead, accessibility loss was highly localised, with a limited number
298 of predominantly rural districts accounting for a disproportionate share of inaccessible facilities. The finding
299 that a small but strategically critical fraction of major road segments became unusable during flood conditions

300 provides an explanation for these patterns, demonstrating that network severance, rather than facility scarcity
301 alone, drove accessibility outcomes [39].

302 Short-range access was most severely affected. At a 5 km threshold, more than three-quarters of healthcare
303 facilities in both Sindh and Punjab were classified as inaccessible, indicating widespread collapse of local access
304 during flood conditions. This finding highlights the sensitivity of short-distance accessibility to disruptions in
305 road connectivity, particularly in settings where alternative routes are limited.

306 Primary care facilities experienced the greatest disruption, whereas secondary and tertiary facilities were
307 generally more accessible due to their concentration near district centres. The disproportionate impact on lower-
308 order road infrastructure, particularly secondary roads serving rural areas, directly contributed to the observed
309 accessibility loss for primary care facilities, which are predominantly located in peri-urban and rural settings.

310 Importantly, districts with large numbers of facilities were not necessarily more resilient, underscoring that
311 healthcare accessibility during floods is governed by network connectivity rather than facility availability alone.
312 Similar patterns have been observed in previous flood events in Pakistan [3]. Disruptions to healthcare access
313 during floods can delay treatment for chronic conditions, maternal care, and routine immunisation, with
314 disproportionate impacts on vulnerable populations [40,41].

315 The strong spatial clustering of both road network disruption and healthcare inaccessibility highlights
316 pronounced inequalities between rural and urban districts. Rural districts in southern and western Punjab and
317 interior Sindh experienced near-total loss of access within commonly used distance thresholds, whereas major
318 urban centres retained substantial connectivity despite geographic exposure to flooding.

319 These contrasts reflect differences in road network structure, particularly the limited redundancy of transport
320 routes in rural areas. Where few alternative paths exist, disruption to even a small number of road segments can
321 isolate entire districts. This pattern further highlights the role of network structure in amplifying accessibility
322 loss under flood conditions. Similar dynamics have been observed in previous studies of flood-related network
323 disruption and accessibility loss [42].

324 These findings highlight structural vulnerabilities in Pakistan's healthcare delivery system during flood
325 emergencies. The disproportionate impact on primary care facilities indicates that first-line health services,
326 which play a critical role in early treatment and referral, are particularly fragile under conditions of network
327 disruption. Floods in Pakistan frequently damage healthcare infrastructure, disrupt medical supply chains, and
328 contaminate water sources, triggering secondary public health crises. During recent flood events, millions of
329 people lacked access to safe drinking water, leading to outbreaks of diarrhoeal disease, while stagnant
330 floodwaters facilitated the spread of malaria and dengue. The World Health Organisation has reported that
331 approximately 10% of healthcare facilities were damaged or destroyed during the 2022 floods, with over 2,000
332 facilities affected in a system where baseline access is already limited. The observation that network
333 fragmentation occurred even in districts with moderate overall road flooding underscores the sensitivity of
334 healthcare accessibility to the failure of strategically located network segments. This finding has important
335 implications for infrastructure planning, suggesting that targeted protection or redundancy at critical road
336 corridors could yield substantial benefits for maintaining healthcare access during flood events.

337 From a planning perspective, these results emphasise the need for district-specific preparedness strategies that
338 prioritise maintaining connectivity to primary care facilities in flood-prone areas. Interventions such as pre-
339 positioned mobile health units, flood-resilient upgrades to critical road segments, and alternative transport

340 planning could substantially reduce accessibility loss during future flood events. This framework could be
341 extended to identify and prioritise critical road segments whose failure would disproportionately affect access,
342 supporting targeted infrastructure investment. Previous studies have demonstrated the utility of network
343 centrality measures for identifying such critical infrastructure, enabling prioritisation of both primary and
344 backup routes. Despite the recurrent and increasingly predictable nature of flooding in Pakistan, disaster
345 response remains largely reactive, with limited emphasis on anticipatory planning. Districts, which are central to
346 operational response, remain among the most neglected administrative tiers in climate preparedness efforts.
347 Strengthening district-level planning, safeguarding essential infrastructure, and ensuring continuity of services
348 such as water, power, and communications are critical to maintaining healthcare functionality during flood
349 events. Locating health facilities on elevated terrain, ensuring secure pharmaceutical storage, and retrofitting
350 existing facilities can further reduce vulnerability to flood-related damage.

351 Importantly, province-level planning alone risks obscuring critical sub-regional vulnerabilities revealed by this
352 analysis. By integrating high-resolution flood extent data with network-based accessibility modelling, this study
353 captures dimensions of healthcare access loss that are not observable through straight-line distance measures or
354 facility counts alone. Euclidean proximity tends to overestimate functional access, particularly in regions with
355 fragmented infrastructure and significant natural barriers [41]. The use of multiple distance thresholds enables
356 interpretation across diverse urban and rural contexts and supports more nuanced planning decisions. The
357 methodological framework is transferable to other flood-prone regions, particularly in LMICs where healthcare
358 access is strongly mediated by road infrastructure and where reliable travel-time data are often unavailable.
359 Similar applications following recent flood events, such as Cyclone Idai in Mozambique, have demonstrated the
360 value of such approaches for identifying critical infrastructure and assessing accessibility loss. As climate
361 change continues to intensify flood hazards and expand the geographic range of disease vectors, health systems
362 in South Asia face increasing strain. Incorporating network vulnerability into disaster risk reduction and health
363 system planning will therefore be essential to reducing preventable health impacts during future flood events.

364 Several limitations should be acknowledged. Travel time and flood depth were not explicitly modelled due to
365 data constraints, and network distance was used as a proxy for accessibility. While this simplifies real-world
366 conditions, it may lead to over- or under-estimation of functional access in areas with variable road conditions or
367 flood severity. In Pakistan's flood context, this is particularly relevant where road surface conditions and flood
368 depth vary significantly, meaning some nominally 'usable' segments may in practice be impassable, suggesting
369 our estimates of accessible facilities could be optimistic. Flood extent was treated as static, and potential
370 behavioural adaptations such as boat travel or informal routes were not considered. The analysis also did not
371 account for facility capacity or service quality. Future research could integrate dynamic flood modelling, travel-
372 time estimation, and facility-level service data to refine accessibility assessments. Linking network disruption
373 directly to health outcomes would further strengthen understanding of the public health consequences of flood-
374 related access loss. Developing multimodal network approaches and further testing network centrality indicators
375 across different hazards and geographic contexts would help advance this field of research.

376 **5 Conclusion**

377 This study provides a spatially explicit assessment of healthcare accessibility during the 2025 monsoon floods in
378 Pakistan. It shows that flood impacts on health systems are strongly mediated by road network disruption and

379 exhibit substantial geographic heterogeneity. While more than one million people were exposed to flooding, the
380 resulting loss of healthcare access was highly localised, with a small number of districts accounting for a
381 disproportionate share of inaccessible facilities.

382 These findings underscore the importance of considering network vulnerability and spatial configuration, rather
383 than facility availability alone, when evaluating health system resilience to flood hazards. From a planning
384 perspective, the results highlight the need for district-specific preparedness strategies that prioritise maintaining
385 connectivity to primary care facilities in flood-prone areas. Interventions such as pre-positioned mobile health
386 units, flood-resilient upgrades to critical road segments, and alternative transport planning may help reduce
387 accessibility loss during future flood events.

388 Network-based accessibility analysis provides a valuable tool for disaster preparedness by identifying critical
389 road segments whose failure would significantly impact population access to healthcare. By combining high-
390 resolution flood extent data with network-based accessibility modelling, this study captures aspects of
391 healthcare access loss that are not observable through straight-line distance measures or facility counts alone.

392 From a policy perspective, this approach enables the identification of priority road segments for targeted
393 intervention, supporting more effective allocation of resources in flood-prone regions. Integrating such analyses
394 into district-level planning can help maintain connectivity to essential healthcare services during extreme events,
395 particularly in LMICs where access is strongly dependent on road infrastructure.

396 **6 Acknowledgements**

397 Not applicable

398 **7 References**

- 399 1. Calvin, K., Dasgupta, D., Krinner, G., Mukherji, A., Thorne, P. W., Trisos, C., Romero, J., Aldunce, P.,
400 Barrett, K., Blanco, G., Cheung, W. W. L., Connors, S., Denton, F., Diongue-Niang, A., Dodman, D.,
401 Garschagen, M., Geden, O., Hayward, B., Jones, C., ... Péan, C. (with Lee, H.). (2023). *IPCC, 2023:*
402 *Climate Change 2023: Synthesis Report. Contribution of Working Groups I, II and III to the Sixth*
403 *Assessment Report of the Intergovernmental Panel on Climate Change [Core Writing Team, H. Lee and J.*
404 *Romero (eds.)]. IPCC, Geneva, Switzerland. Intergovernmental Panel on Climate Change.*
405 <https://doi.org/10.59327/ipcc/ar6-9789291691647>
- 406 2. Atta-ur-Rahman, & Khan, A. N. (2013). Analysis of 2010-flood causes, nature and magnitude in the
407 Khyber Pakhtunkhwa, Pakistan. *Natural Hazards*, 66(2), 887–904. [https://doi.org/10.1007/s11069-012-](https://doi.org/10.1007/s11069-012-0528-3)
408 0528-3
- 409 3. Iqbal, A., Nazir, H., & Khurshid, N. (2024). Exploring the effects of floods in Pakistan: Pre/post flood
410 analysis 2022. *International Journal of Disaster Risk Reduction*, 115, 105032.
411 <https://doi.org/10.1016/j.ijdr.2024.105032>

- 412 4. Tanveer Piracha & Huda Kamal. (2025). *A Comprehensive Study of Flood Events in Pakistan 1950-2025*
413 (National Institute of Disaster Management (NIDM) Publication). National Disaster Management Authority
414 (NDMA), Government of Pakistan.
415 <https://www.ndma.gov.pk/storage/publications/September2025/5a7DeS9RPoaFUxreIcmm.pdf>
- 416 5. Lutz, A. F., Immerzeel, W. W., Shrestha, A. B., & Bierkens, M. F. P. (2014). Consistent increase in High
417 Asia's runoff due to increasing glacier melt and precipitation. *Nature Climate Change*, 4(7), 587–592.
418 <https://doi.org/10.1038/nclimate2237>
- 419 6. Zafar, Z., Nadeem, A. A., Zha, Y., Gilani, H., & Tariq, A. (2025). Snow cover variability assessment and its
420 interplay with hydro-climatic characteristics in data scarce region of Gilgit-Baltistan, Pakistan. *Journal of*
421 *Environmental Management*, 382, 125375. <https://doi.org/10.1016/j.jenvman.2025.125375>
- 422 7. Ali, M., & Mahmood, S. (2024). Geo-spatial assessment of pluvial floods in city district Lahore, Pakistan.
423 *Environmental Monitoring and Assessment*, 196(2), 189. <https://doi.org/10.1007/s10661-023-12291-6>
- 424 8. Sadiq, M., Eqani, S. A. M. A. S., Podgorski, J., Ilyas, S., Abbas, S. S., Shafqat, M. N., Nawaz, I., & Berg,
425 M. (2024). Geochemical insights of arsenic mobilization into the aquifers of Punjab, Pakistan. *Science of*
426 *The Total Environment*, 935, 173452. <https://doi.org/10.1016/j.scitotenv.2024.173452>
- 427 9. Khan, G., Ali, S., Xiangke, X., Qureshi, J. A., Ali, M., & Karim, I. (2021). Expansion of Shishper Glacier
428 lake and recent glacier lake outburst flood (GLOF), Gilgit-Baltistan, Pakistan. *Environmental Science and*
429 *Pollution Research*, 28(16), 20290–20298. <https://doi.org/10.1007/s11356-020-11929-z>
- 430 10. Portalés-Julià, E., Mateo-García, G., Purcell, C., & Gómez-Chova, L. (2023). Global flood extent
431 segmentation in optical satellite images. *Scientific Reports*, 13(1), 20316. <https://doi.org/10.1038/s41598-023-47595-7>
- 432
- 433 11. Qamer, F. M., Abbas, S., Ahmad, B., Hussain, A., Salman, A., Muhammad, S., Nawaz, M., Shrestha, S.,
434 Iqbal, B., & Thapa, S. (2023). A framework for multi-sensor satellite data to evaluate crop production
435 losses: The case study of 2022 Pakistan floods. *Scientific Reports*, 13(1), 4240.
436 <https://doi.org/10.1038/s41598-023-30347-y>
- 437 12. Tatem, A. J. (2017). WorldPop, open data for spatial demography. *Scientific Data*, 4(1), 170004.
438 <https://doi.org/10.1038/sdata.2017.4>
- 439 13. Tellman, B., Sullivan, J. A., Kuhn, C., Kettner, A. J., Doyle, C. S., Brakenridge, G. R., Erickson, T. A., &
440 Slayback, D. A. (2021). Satellite imaging reveals increased proportion of population exposed to floods.
441 *Nature*, 596(7870), 80–86. <https://doi.org/10.1038/s41586-021-03695-w>

- 442 14. Pebesma, E., & Bivand, R. (2023). *Spatial Data Science: With Applications in R* (1st edn). Chapman and
443 Hall/CRC. <https://doi.org/10.1201/9780429459016>
- 444 15. Pebesma, E. (2018). Simple Features for R: Standardized Support for Spatial Vector Data. *The R Journal*,
445 *10*(1), 439. <https://doi.org/10.32614/RJ-2018-009>
- 446 16. Hijmans, R. J. (2020). *terra: Spatial Data Analysis* (p. 1.8-93) [Data set].
447 <https://doi.org/10.32614/CRAN.package.terra>
- 448 17. Van Der Meer, L., Abad, L., Gilardi, A., & Lovelace, R. (2021). *sfnetworks: Tidy Geospatial Networks* (p.
449 0.6.5) [Data set]. <https://doi.org/10.32614/CRAN.package.sfnetworks>
- 450 18. Wickham, H., François, R., Henry, L., Müller, K., & Vaughan, D. (2014). *dplyr: A Grammar of Data*
451 *Manipulation* (p. 1.1.4) [Data set]. <https://doi.org/10.32614/CRAN.package.dplyr>
- 452 19. Wickham, H., Vaughan, D., & Girlich, M. (2014). *tidyr: Tidy Messy Data* (p. 1.3.2) [Data set].
453 <https://doi.org/10.32614/CRAN.package.tidyr>
- 454 20. R Core Team. (2025). *R: A Language and Environment for Statistical Computing* [Computer software]. R
455 Foundation for Statistical Computing. <https://www.R-project.org/>
- 456 21. QGIS Development Team. (2025). *QGIS Geographic Information System: 3.40.9* [Computer software].
457 Open Source Geospatial Foundation. <https://qgis.org>
- 458 22. UNITAR, U. (2025). *Satellite-detected water extents in Punjab Province, Pakistan as of 10 July 2025*
459 [Map]. United Nations Institute for Training and Research (UNITAR). <https://unosat.org/products/4147>
- 460 23. UNITAR, U. (2025). *Satellite-detected water extents in Sindh, Balochistan and Punjab Provinces, Pakistan*
461 *as of 11 July 2025* [Map]. United Nations Institute for Training and Research (UNITAR). [https://unosat.org/](https://unosat.org/products/4147)
462 [products/4147](https://unosat.org/products/4147)
- 463 24. OpenStreetMap contributors. (2026). *Pakistan Roads* [Data set]. Humanitarian Data Exchange.
464 https://data.humdata.org/dataset/hotosm_pak_roads
- 465 25. OpenStreetMap contributors. (2026). *Pakistan Health Facilities* [Data set]. Humanitarian Data Exchange.
466 https://data.humdata.org/dataset/hotosm_pak_health_facilities
- 467 26. World Food Programme SDI. (2025). *Pakistan Subnational Administrative Boundaries* [Data set].
468 Humanitarian Data Exchange. <https://data.humdata.org/dataset/cod-ab-pak>
- 469 27. Papilloud, T., Steiner, A., Zischg, A., & Keiler, M. (2024). Road network disruptions during extreme
470 flooding events and their impact on the access to emergency medical services: A spatiotemporal

- 471 vulnerability analysis. *Science of The Total Environment*, 956, 177140.
472 <https://doi.org/10.1016/j.scitotenv.2024.177140>
- 473 28. Petricola, S., Reinmuth, M., Lautenbach, S., Hatfield, C., & Zipf, A. (2022). Assessing road criticality and
474 loss of healthcare accessibility during floods: The case of Cyclone Idai, Mozambique 2019. *International*
475 *Journal of Health Geographics*, 21(1), 14. <https://doi.org/10.1186/s12942-022-00315-2>
- 476 29. He, K., Carhart, N., Pregolato, M., Neal, J., & De Risi, R. (2026). Probabilistic functionality assessment of
477 road networks for medical emergency vehicles during flooding. *Natural Hazards*, 122(6), 233.
478 <https://doi.org/10.1007/s11069-026-08005-z>
- 479 30. Kramer, M., Terheiden, K., & Wieprecht, S. (2016). Safety criteria for the trafficability of inundated roads
480 in urban floodings. *International Journal of Disaster Risk Reduction*, 17, 77–84.
481 <https://doi.org/10.1016/j.ijdrr.2016.04.003>
- 482 31. Nesbitt, R. C., Gabrysch, S., Laub, A., Soremekun, S., Manu, A., Kirkwood, B. R., Amenga-Etego, S.,
483 Wiru, K., Höfle, B., & Grundy, C. (2014). Methods to measure potential spatial access to delivery care in
484 low- and middle-income countries: A case study in rural Ghana. *International Journal of Health*
485 *Geographics*, 13(1), 25. <https://doi.org/10.1186/1476-072X-13-25>
- 486 32. Rachmawati, D., & Gustin, L. (2020). Analysis of Dijkstra's Algorithm and A* Algorithm in Shortest Path
487 Problem. *Journal of Physics: Conference Series*, 1566(1), 012061. [https://doi.org/10.1088/1742-](https://doi.org/10.1088/1742-6596/1566/1/012061)
488 [6596/1566/1/012061](https://doi.org/10.1088/1742-6596/1566/1/012061)
- 489 33. Javaid, M. A. (2013). Understanding Dijkstra Algorithm. *SSRN Electronic Journal*. [https://doi.org/10.2139/](https://doi.org/10.2139/ssrn.2340905)
490 [ssrn.2340905](https://doi.org/10.2139/ssrn.2340905)
- 491 34. Dijkstra, E. W. (1959). A note on two problems in connexion with graphs. *Numerische Mathematik*, 1(1),
492 269–271. <https://doi.org/10.1007/BF01386390>
- 493 35. Tegegne, T. K., Chojenta, C., Loxton, D., Smith, R., & Kibret, K. T. (2018). The impact of geographic
494 access on institutional delivery care use in low and middle-income countries: Systematic review and meta-
495 analysis. *PLOS ONE*, 13(8), e0203130. <https://doi.org/10.1371/journal.pone.0203130>
- 496 36. Gabrysch, S., Cousens, S., Cox, J., & Campbell, O. M. R. (2011). The Influence of Distance and Level of
497 Care on Delivery Place in Rural Zambia: A Study of Linked National Data in a Geographic Information
498 System. *PLoS Medicine*, 8(1), e1000394. <https://doi.org/10.1371/journal.pmed.1000394>
- 499 37. Bradley, D. R., & Cutcomb, S. (1977). Monte Carlo simulations and the chi-square test of independence.
500 *Behavior Research Methods & Instrumentation*, 9(2), 193–201. <https://doi.org/10.3758/BF03214499>

- 501 38. Loreti, S., Ser-Giacomi, E., Zischg, A., Keiler, M., & Barthelemy, M. (2022). Local impacts on road
502 networks and access to critical locations during extreme floods. *Scientific Reports*, *12*(1), 1552.
503 <https://doi.org/10.1038/s41598-022-04927-3>
- 504 39. Ulasan, A., & Ergun, O. (2018). Restoration of services in disrupted infrastructure systems: A network
505 science approach. *PLOS ONE*, *13*(2), e0192272. <https://doi.org/10.1371/journal.pone.0192272>
- 506 40. Sankam, J., Rao, A. P., Sumit, K., & Tiwari, R. R. (2023). Role of Natural and Anthropogenic Factors in
507 Causing Frequent Floods in Assam, India: A Scoping Review. *International Journal of Environmental*
508 *Health Engineering*, *12*(5). https://doi.org/10.4103/ijehe.ijehe_58_22
- 509 41. Xia, T., Song, X., Zhang, H., Song, X., Kanasugi, H., & Shibasaki, R. (2019). Measuring spatio-temporal
510 accessibility to emergency medical services through big GPS data. *Health & Place*, *56*, 53–62.
511 <https://doi.org/10.1016/j.healthplace.2019.01.012>
- 512 42. Freiria, S., Tavares, A. O., & Pedro Julião, R. (2015). The Multiscale Importance of Road Segments in a
513 Network Disruption Scenario: A Risk-Based Approach. *Risk Analysis*, *35*(3), 484–500.
514 <https://doi.org/10.1111/risa.12280>

515 **8 Declarations**

516 **Funding:** No funding was received for this research.

517 **Ethics approval and consent to participate:** Not applicable.

518 **Consent to Publish declaration:** Not applicable.

519 **Data Availability:** All the data is available online and can be accessed via the links/sources provided in the data
520 section.

521 **9 Conflict of interest:**

522 The authors declare that they have no conflict of interest.